Geochemical characteristics of suspended particulate matter around Piscadera Bay and its influence on nearshore ecosystems, Curaçao (Caribbean Sea)

Virginia Sánchez Barranco[1*]; Nienke C.J. van de Loosdrecht[2]; Furu Mienis[1]; Jasper M. de Goeij[2]; Rick Hennekam[1]; Gert-Jan Reichart[1,3]; Jan-Berend W. Stuut[1,4]; Lennart J. de Nooijer[1]

[1] Royal Netherlands Institute for Sea Research (NIOZ), department of Ocean Systems, Den Burg, the Netherlands.

[2] Department Freshwater and Marine Ecology (FAME), Institute for Biodiversity and Ecosystem Dynamics (IBED), University of Amsterdam, Amsterdam, the Netherlands.

[3] Department of Earth Sciences, Faculty of Geosciences, Utrecht University, Budapestlaan 4, 3584 CD Utrecht, the Netherlands.

[4] Vrije Universiteit Amsterdam (VU Amsterdam), Faculty of Science, Department of Earth Sciences, Amsterdam, the Netherlands.

*Corresponding author

Abstract. Caribbean coral reefs face rising pressure from coastal development, yet the pathways by which urban pollution reaches these endangered ecosystems remain poorly understood. Bays act as dynamic channels, trapping, transforming, and releasing matter that can impact adjacent reef systems. We investigated the temporal and spatial variability of suspended particulate matter (SPM), a key vector for pollutants and nutrients, derived from an urbanized bay in Curaçao and determined their effect on surrounding coral reefs. Using sediment traps deployed across spatial gradients (bay mouth to nearby reefs in the East and West) during the dry (April-May) and wet (October-November) seasons in 2023, we measured mass, carbon, and nitrogen fluxes and associated grain-size and geochemical particle composition. Results were compared to environmental conditions (e.g. rainfall, current speed) and revealed a clear spatial gradient of bay influence: the bay mouth showed the strongest terrestrial signal with highest mass fluxes, followed by the eastern reef (sheltered from currents) with elevated SPM and carbon fluxes of fine particles enriched in terrigenous elements (Si, Fe, Al, and Mn), while the western reef (exposed to open-ocean flow) exhibited lower fluxes of coarser particles with elevated Ca/Fe, Pb, Cu and Ni. This indicates a diminished bay effect and stronger marine influence mixed with localized pollution. During the dry

season, differences in SPM fluxes and composition between reef sites were minimal, but wet season conditions amplified spatial patterns, with rainfall-driven runoff locally increasing dissolved and particulate matter delivery. This implies that reef vulnerability to bay-derived pollution locally depends on both proximity to source waters and seasonal hydrodynamic variability, with sheltered reefs experiencing the greatest impacts during periods of enhanced terrestrial runoff.

Key words: SPM, Coral reefs, Terrestrial runoff, Spatial gradient, Seasonal variability, Carbon flux

1. Introduction

In recent decades, land-use changes and coastal development around watersheds have increased runoff of sediments, nutrients and chemical pollutants into tropical coastal waters, posing significant threats to coral reefs worldwide, including those in the Caribbean (Burke and Maidens, 2004; Burke et al., 2011). The accumulation of terrestrial discharge on nearshore reefs causes local changes to reef communities, for example the increased cover of (macro) algae (Fabricius, 2005) or suffocation of corals (Weber et al., 2006). Local stressors also make them more vulnerable to global ones, such as thermal bleaching and ocean acidification due to compounded energy deficits and impaired recovery pathways (Storlazzi et al., 2015; Dutra et al., 2018; Anthony et al., 2008). Inland bays on Caribbean islands could play an important role in the supply of sediments, nutrients and pollutants. They show strong environmental variability (diel and seasonal) in physicochemical parameters and higher nutrient and pollutant concentrations compared to reef waters (de Jong et al., 2025), and serve as locations where land-derived substances are retained, transformed, or exported to coastal waters (Heiskanen and Tallberg, 1999). In tropical island environments, discharge from bays is typically episodic, occurring mainly during the rainy season and storm events leading to pulses of material and runoff being released into the ocean (Ringuet and Mackenzie, 2005; De Carlo et al., 2007; Sánchez Barranco et al., 2025; Larson et al., 2015).

Suspended particulate matter (SPM) plays a key role in the transport and cycling of minerals, organic matter, nutrients, and pollutants, all of which can influence coral reef health (Jouon et al., 2008). For example, sediment plumes, often dominated by fine-grained material, can reduce light availability and physically stress coral reefs, especially near river mouths and coastal bays (Fabricius, 2005; Ramos-Scharrón and Macdonald, 2005). Sedimentation from SPM can also physically smother coral polyps, impair recruitment, and increase mortality (Bhuyan et al., 2025; Erftemeijer et al., 2012). The energetic cost of shedding sediments—via mucus production and ciliary action—can further compromise coral metabolism and resilience (Tuttle and Donahue, 2022). Some studies also show that certain reef organisms can benefit from SPM. For instance, soft corals may utilize detritus and other small SPM (<10 µm particle size) as an important food source, particularly in high-turbidity environments (Anthony, 1999; Fabricius and Dommisse, 2000). De Jong et al. (2025) have shown that the environmental conditions in semi-enclosed bays, where coral communities often persist, can be highly variable compared to open reefs. Reduced light penetration due to suspended sediments limits the photosynthetic energy available for coral growth and reproduction, with finer-grained and darker-coloured sediments causing more pronounced effects than coarser, lighter ones (Anthony and Fabricius, 2000; Weber et al., 2006; Storlazzi et al., 2015). In addition, fine-grained SPM remains longer in suspension, leading to prolonged elevated levels of turbidity. Beyond its impact on light availability, SPM also plays a crucial role in pollutant dynamics. Heavy metals and organic contaminants readily bind to SPM, particularly clays and silts, making them a critical vector for pollutant transport in near-shore marine environments (Salomons and Förstner, 2012; Zhang et al., 2018). This is of particular concern in the Caribbean, where metal pollution poses ecological risks due to its persistence in reef ecosystems (Berry et al., 2013; Guzmán and Jiménez, 1992).

The south coast of Curaçao is characterized by several inland bays that may contribute to the transport of particulate substances to nearby coastal ecosystems, including coral reefs, mangroves, and seagrass beds (Debrot et al., 1998; Wagenaar Hummelinck, 1977). Despite a 50% loss in coral cover over the past 50 years (Sandin et al., 2022) the reefs along the south coast of Curaçao (southeastern Caribbean) are still considered among the healthiest in the Caribbean Sea (Sandin et al., 2008a; Rijsberman and Westmacott, 2000; Sandin et al., 2022; Jackson et al., 2014). Seasonal bay-ocean exchange dynamics are influencing the water-column characteristics of nearby coastal ecosystems (Sánchez Barranco et al., 2025). In Curaçao, bay–ocean exchange is limited during the dry season, leading to the build-up of nutrient concentrations within the bays, whereas during the wet season, increased mixing between bay and offshore waters is enhanced (Sánchez Barranco et al., 2025). These dynamic exchange processes potentially create a complex mechanism for sediment and nutrient transfer between coastal environments. However, while it is known that bays release SPM into surrounding waters (Restrepo et al., 2016; D'sa and Ko, 2008), the extent of its distribution, deposition, and seasonal variability, and its effect on changes in benthic composition, remain poorly quantified.

Here, we aim to quantify fluxes of SPM and assess their geochemical characteristics in proximity and further away from a bay located on the Caribbean Island Curaçao. The coastal zone near Piscadera Bay, located on the south coast of Curaçao, has been studied extensively and has one of the longest benthic cover records in the world (De Bakker et al., 2017) providing a unique site to study the potential influence of bay discharge on nearby reefs. We present a study in which sediment traps were deployed for 30 days at various locations around Piscadera Bay during April/May 2023 (dry season) and October/November 2023 (wet season). Temporal variability in SPM fluxes, sampled in the dry and wet seasons, was compared to environmental conditions (e.g. rainfall, wind, tides) to determine if they explain the observed spatio-temporal variability in SPM fluxes and composition. Collected material was analyzed for grain size, elemental, and organic matter composition.

2. Methodology

2.1 Study site

The island of Curaçao lies near the Venezuelan coast with a surface area of approximately 444 km^2 and around 150.000 inhabitants and around 1.2 million (cruise) tourists visit the island annually. The south coast is bordered by fringing reefs that start at a water depth of approximately 7 m followed by a steep slope down to 30–50 m (Bak, 1977; De Bakker et al., 2016). The island is characterized by a semi-arid climate, including a wet season with highest precipitation rates in the months of October-December (ranging between 80-115 mm per month) and a dry season with lowest monthly rainfall in April-June (ranging between 8-15 mm per month) (Wit et al., 2025).

This study focuses on Piscadera Bay (Fig. 1), an area that serves as an important catchment area, draining 16–17 km^2 of the mid-west part of the island of Curaçao (Sánchez Barranco et al., 2025). The bay’s wide mouth (ranging from 76 m at its narrowest point to 105 m at its widest) has a shallow entrance of less than 6 m deep. Originally, Piscadera Bay opened to the sea through a narrow, shallow channel, mostly blocked by a coral and debris bar, with a cross-sectional area of only 7 m². In 1962, the entrance was widened to 45 m², and in the early Seventies it was further enlarged and deepened (Hofker, 1971).

The reef sites surrounding the bay reflect significant ecological changes over time (Sandin et al., 2022; De Bakker et al., 2017). The reef west of the bay's mouth, which has experienced substantial coral degradation, showed 8.2% hard coral cover in 2015, compared to an estimated 40% in 1982, with 29.7% turf cover and 2.7% cyanobacterial mats in 2015 (Sandin et al., 2022; Van Duyl, 1985). The reef directly east of Piscadera's mouth also experienced an ecological transformation, with hard coral cover declining from an estimated 5% in 1982 to merely 0.9% in 2015, accompanied by 51.5% turf cover and 11.5% cyanobacterial mats (De Bakker et al., 2016; Van Duyl, 1985; Sandin et al., 2022).

Fieldwork was conducted in 2023 in April–May (dry season) and October–November (wet season). Sediment traps were deployed for 30 days at the mouth of the bay (3–5 m water depth), at the east reef side at 8 and 18 m water depth and at the west reef side of the bay at 8 and 18 m water depth (Fig. 1). At each site, 6 traps were deployed at least 1 m apart from each other following Storlazzi et al. (2011).

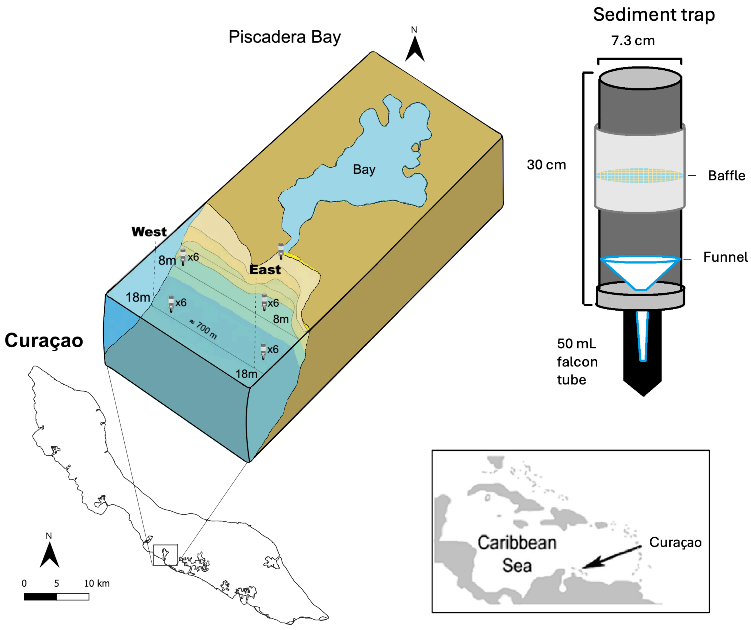

Figure 1. Map of Curaçao showing the studied location of Piscadera Bay on the west side of Willemstad. The inset provides a detailed sketch of the study area around Piscadera Bay, with sediment traps deployed at the bay mouth and at eastern and western reef sites, each sampled at two water depths (8 m and 18 m). The sediment traps used, follow the design recommendations of Storlazzi et al. (2011) and an example is shown on the right side for reference.

2.2 Current sensors and environmental data

In October–November 2023, two Acoustic Doppler Current Profilers (ADCP) were deployed at a depth of 10 m at the eastern and western reef of Piscadera Bay for a 30-d period. In April–May 2023, the ADCPs were also deployed for shorter periods of time at the mouth (7 d), eastern (4 d), and western reef (20 d). The ADCPs were used to measure current speed and direction, water temperature, and pressure, which was used to determine tidal cycles. Water speed and direction data used in this study were taken from ADCP bin 3 located 2 m above the seafloor, which corresponded to 8 m water depth at the reef sites (with a total water depth of 10 m) and 3 m water depth near the mouth of the bay (with a total water depth of 5 m). Precipitation and wind data during the sampling periods were retrieved from the Meteorological Department of Curaçao (Meteorological Department Curaçao, n.d.).

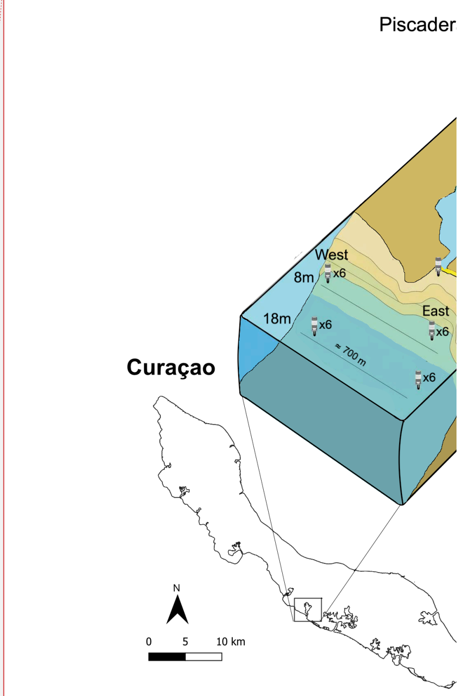

Deleted:

Deleted:

Deleted: at water depths of 8 m and 18 m.

2.3 Sediment traps and mass fluxes

Sediment traps were built following Storlazzi et al. (2011), with a height of 30 cm, and a surface area of 41.85 cm^2 to collect gross particle fluxes. In shallow, energetic reef environments sediment traps will collect settling lateral transported and resuspended bottom particles. Traps (*n* =6 per site and depth) were secured with a steel rebar into the sediments with their mouths at 0.7–0.8 m above the seafloor. Inside the trap a baffle was placed to avoid organisms or large objects from entering the funnel. At the bottom of the trap, a funnel connected to a 50 mL dark falcon tube was used to collect suspended particulate matter. In April–May 2023, traps at the mouth of the bay were sampled every 5 d and the ones in the eastern and western reef every 10 d. In October–November 2023, Falcon tubes were replaced every 5 d at each location. After collection, samples were centrifuged and excess water was removed, frozen in a -20 °C freezer and freeze-dried to be transported to the Netherlands for further analysis. To remove seawater salts, the freeze-dried samples were resuspended in Milli-Q water, centrifuged again, and the supernatant was carefully pipetted out, after which samples were freeze-dried again. Freeze-dried samples were weighed with a high-precision microbalance (±0.1 mg resolution), and an uncertainty of ± 0.0001 g was applied to all mass measurements. Carbon and nitrogen percentages were measured with a precision of ± 0.02%. These uncertainties were propagated through all derived fluxes, resulting in mass flux values reported to two decimal places, and C_{org} and total N flux values reported to two and three decimal places, respectively. Grain-size measurements and silt/clay percentages were obtained using laser diffraction, with instrument precision better than 1 µm and 0.1%, respectively. The final calculated grain-size measurements and silt/clay percentages are reported to two decimal places.

2.4 Organic carbon and nitrogen content

Organic carbon and total nitrogen contents were measured using an Elementar Vario El Cube elemental analyzer (EA; Elementar Analysensysteme GmbH, Germany) coupled to an Isoprime vision isotopic ratio mass spectrometer (IRMS; Elementar Analysensysteme, GmbH, Germany) at the University of Amsterdam. Prior to analysis, dried suspended particulate matter from the traps was ground using an agate mortar and pestle to homogenize. Subsequently, samples were transferred into silver cups and weighed. The day before measuring, inorganic carbonates were removed by repeated treatment with 1 mol L^{-1} hydrochloric acid until effervescence stopped. The silver cups were dried overnight on a heating plate and closed the following day with tweezers. For carbon and nitrogen content analyses, three out of the six replicates collected per location and time point were randomly selected for measurements.

2.5 Grain-size analysis

Grain-size analyses were conducted using a Beckman Coulter laser diffraction particle sizer LS13 320. Prior to analysis, 2 mL of sodium pyrophosphate ($Na_4P_2O_7 \cdot 10\,H_2O$) was added to each sample, followed by brief sonication for 10 min to ensure complete disaggregation of any remaining particle aggregates. Degassed water was used during the analysis to reduce the impact of gas bubbles, and a magnetic stirrer was used to keep the sample homogenized. The particle-size distributions were categorized into 92 size classes, ranging from 0.375 to 2,000 µm following Van Der Does et al. (2016). Testing with internal glass-bead standards demonstrated a reproducibility of better than 0.7 µm for mean particle size and 0.6 µm for median particle size (1σ). The average standard deviation across all size classes was within 4 vol.%.

2.6 XRF elemental analysis

X-ray Fluorescence (XRF) was employed as a non-destructive method to assess elemental composition in SPM samples, performed with an Avaatech scanner at NIOZ. Sub-samples (triplicate) were taken from the Milli-Q-washed, freeze-dried sediment trap samples (see Section 2.3) and homogenized and ground with a pestle and mortar to a fine particle size. The samples were placed in sample holders with a 6 mm radius, following the procedure of Korte et al. (2017). The XRF analysis was carried out using two energy settings: 10 kV for aluminum (Al), silicon (Si), sulfur (S), iron (Fe), and manganese (Mn), and 30 kV for nickel (Ni), bromine (Br), and lead (Pb). For the 10 kV measurements, a current of 1500 µA was applied for 20 seconds without a filter, while the 30 kV measurements used a 500 µA current for 20 seconds with a palladium filter to optimize detection. To check precision of our analyses, one external reference standard (SARM 2) was measured repeatedly and we calculated the coefficient of variation (CV%) per element for one of the standards (SARM 2), which was consistently below 4%. Each sample was analyzed three times to assess internal variability. Data was processed using bAxil spectrum analysis software (developed by Brightspec).

2.7 Statistical analysis

First, outliers of mass, carbon, and nitrogen fluxes were identified and removed following robust statistical methods for outlier detection, using the median absolute deviation (MAD) approach as described by Rousseeuw and Hubert (2011). This resulted in the removal of 15 mass flux values out of 274 datapoints (5.5 %). These outliers corresponded to exceptionally low fluxes, which were caused by physical obstruction, specifically, shells clogging the sediment trap funnels and preventing material from entering the collection tubes, as observed during sample retrieval. We used the two-sample t-test (independent samples t-test) to compare the means of mass, carbon and nitrogen fluxes, grain size and silt and clay % between wet and dry seasons for each location separately. Prior to analysis, data were checked for normality using the Shapiro–Wilk test and visually assessed using Q-Q plots. Most variables were not normally distributed. For non-normally distributed variables, we applied the non-parametric Kruskal–Wallis test followed by pairwise Wilcoxon rank-sum tests with Bonferroni correction. For normally distributed variables, we used one-way ANOVAs followed by Tukey's Honest Significant Difference (HSD) post-hoc tests to assess differences between locations in the dry and wet seasons. These analyses were conducted separately for each season and applied to grain size, as well as mass, C_{org}, and total N fluxes. Statistical significance was determined using a threshold of $p < 0.05$.

Elemental counts obtained from XRF analysis were normalized to account for variability in physical material properties (e.g., density) and measurement conditions (e.g., detector live time). Normalization was performed by calculating centered log-ratios (CLR) of elemental intensities, following the method described by Bertrand et al. (2024). This approach addresses non-linear matrix effects and ensures comparability between measurements. The CLR transformation involves dividing the intensity of each element by the geometric mean of intensities of all selected elements from the same measurement. The geometric mean is calculated as:

$$g(z) = \left(Counts_{Element\ A\ (z)} * Counts_{Element\ B\ (z)} * \ldots Counts_{Element\ n\ (z)}\right)^{1/n}$$

Deleted: √

where *n* is the total number of selected elements. The CLR value for a specific element is then computed as:

$$CLR\ A\ (z) = \ln\left[\frac{Counts\ Element\ A(z)}{g\ (z)}\right]$$

Only well-measured elements free of noise and zero values were included in the CLR transformation. Principal Component Analysis (PCA) was then performed on the CLR-transformed elemental data to identify the dominant geochemical processes contributing to differences in sediment composition. Element loadings were used to identify groups of elements with high contributions to the total variance along the first two principal components (PC1 and PC2) using a scree plot. To account for the potential impact of differences in dilution due to a variable terrigenous input, trace metals (e.g., Pb, Ni, Y, Rb and Cu) were not CLR-transformed, but instead expressed as the Ln of ratios to Al (e.g., Ln (Pb/Al), Ln (Ni/Al)) (Weltje and Tjallingii, 2008). For visualization, average cluster values were calculated per location and season.

To explore the relationship between SPM characteristics and environmental processes across locations and seasons, a Redundancy Analysis (RDA) was performed. In this analysis, response variables (i.e. mass, C_{org} and total N fluxes, grain size, silt and clay % and CLR of elemental intensities) were modeled as a function of explanatory variables (e.g., rainfall, wind speed, wind direction, distance from land and from the bay mouth). For this analysis, East 8 m and 18 m were combined as 'East,' and West 8 m and 18 m were combined as 'West,' since no consistent depth-related differences were observed. For the multivariate RDA, however, depth was retained as a continuous explanatory variable (5, 8, or 18 m) alongside distance to land and distance to mouth, to explore how spatial gradients jointly relate to compositional variation. Before performing the RDA, Variance Inflation Factors (VIFs) for all explanatory variables in the RDA were calculated to assess collinearity among predictors. All VIFs were below 3 (range: 1.30–2.79), indicating no problematic collinearity. All variables were auto-scaled and mean-centered, and as suggested by Shrestha and Kazama (2007), only RDAs with eigenvalues greater than 1 were considered significant. Additionally, a k-means clustering algorithm was applied to the site scores, revealing distinct groups within the dataset.

Deleted: the locations East 8m and 18 m were combined as East, and West 8 m and 18 m were combined as West, as there were no clear differences between the different depths when examining the RDA results...

Deleted:

Deleted: correlations among explanatory variables were assessed, and highly correlated variables were removed to reduce multicollinearity...

In addition, we determined the relationships between various environmental and SPM variables, by conducting a Spearman correlation analysis for three locations (East, West, and Mouth) within the study area using data of the wet and dry season. Spearman correlations were chosen as most of the variables were not normally distributed. The variables included CLR of elemental intensities, SPM properties (i.e. grain size, silt and clay ratio, mass, C_{org} and total N fluxes), and environmental factors (i.e. rainfall, wind speed and direction and depth).

We categorized correlation (Spearman's rho, r_s) strengths as strong ($r_s > 0.6$) and very strong ($r_s > 0.8$), while weak to moderate correlations were excluded from the visualizations. All statistical analyses and graphing were performed in R (R CoreTeam 2012) using R Studio (R StudioTeam 2015).

3. Results

3.1 Environmental parameters: seasonal and spatial differences

Environmental data revealed distinct differences between the two different sample periods (Fig. 2). During April–May, water temperatures at 10 m water depth of the eastern and western reef varied between 26.5–28.8°C, with the highest temperatures observed between April 24 and May 2, coinciding with the transition from spring tide to neap tide. Rainfall during this period was minimal, with only two notable events: 4 mm on May 14 and 2 mm on May 22. In contrast, the October–November 2023 period showed higher water temperatures, exceeding 30°C from October 28 to November 11 and averaging approximately 29°C throughout the rest of November. Rainfall was substantially higher than in April-May, with precipitation recorded on nearly every sampling day. Based on the rainfall data we refer to the April-May period as dry season and October-November as wet season. The most intense rainfall event occurred between October 25 and November 6, peaking at 24 mm on November 2. Wind also showed distinct seasonal patterns. The period spanning April-May was characterized by consistent southeasterly winds with high average speeds of 20 m s^{-1}, reaching peaks of 27.4 m s^{-1}. October-November exhibited more variable wind directions, predominantly from the southeast, with occasional extreme shifts (e.g., the change in direction recorded on November 20). During October-November wind speeds were notably lower, averaging around 15 m s^{-1}, particularly in early October, though they increased by mid-November. The wet season also showed a relationship between precipitation events and wind patterns, with lower wind speeds often coinciding with heavier rainfall.

The ADCP data revealed spatial variations in water flow between the eastern and western reefs in October-November (Fig. 2). Current velocities were notably higher at the western reef, ranging from 0.01 to 0.07 m s^{-1}, compared to the eastern reef, where velocities ranged mostly from 0.005 to 0.02 m s^{-1}. At the western reef, the prevailing current direction was west-southward. In contrast, the eastern reef exhibited a more variable and diffuse flow pattern, with no clear dominant current direction. Although limited data in April-May prevented robust seasonal comparisons, current speeds showed similar ranges across both seasons.

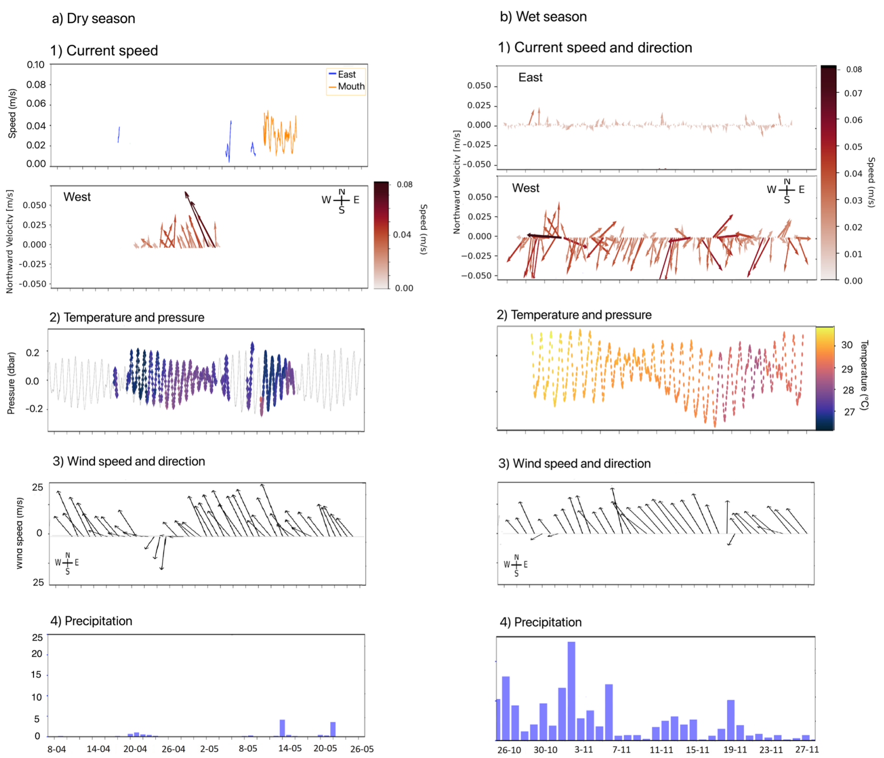

Figure 2. Environmental variables during the sampling periods in a) April-May (dry season) and b) October-November (wet season) 2023. 1) show current speed and direction over time at the western reef site at 8 m, eastern reef site at 8 m and mouth at 3 m. 2) water pressure at 10 m in the reef in dbar (reflecting tidal cycles) and water temperature in °C, the latter represented by a color scale. Panels 3) wind speed (color of the vectors) and direction. Panels 4) show rainfall (mm).

3.2 Seasonal and spatial averages of fluxes and grain size

Properties of SPM showed clear spatial and temporal patterns (Table 1). In April-May, fluxes (total mass, organic carbon (C_{org}), and total N) were significantly higher at the mouth than at the reef locations (Tables 1, S1). In the western reef, SPM had a larger grain size (with a significantly lower proportion of silt and clay) compared to the east and the mouth (Tables 1, S1). In the wet season, the mouth exhibited the highest fluxes, with higher silt and clay contents compared to the material found at the other locations (Table S1). At most sites, mass, C_{org} and total N fluxes were higher in October-November compared to April-May, except for west 18 (Table S2). The mouth showed the strongest seasonal signal: fluxes were 3–4 times higher in October-November and grain size was significantly smaller than in April-May (Table 1, S2).

At the east reef, seasonal differences were also evident, especially at 8 m, where mass fluxes doubled, and C_{org} and total N fluxes increased fourfold in October-November. At 18 m, this seasonal increase in fluxes was more modest, but still clear (Table S2).

Western reefs showed a mixed pattern. At 8 m, fluxes increased in October-November, while at 18 m, they were higher in April-May, contrasting with the other locations. Nonetheless, average grain size was smaller, and silt and clay contents were higher in October-November across all reef sites (i.e. eastern and western reef; Table 1, S1, S2). In particular, during April-May, the western reef had the lowest portion of silt and clay (28–38%), which was significantly lower than at the eastern reef (51–53%).

Table 1. Summary of the mean (highest between seasons per site in bold), maximum and minimum values of mass, C_{org} and total N fluxes (g m^{-2} d^{-1}), grain size (µm), silt and clay % measured at the mouth east 8 and 18 m, and west 8 and 18 m during April-May (dry season) and October-November (wet season). Asterisks show significant differences between seasons (See Tables S1 and S2 for full statistical analyses between locations and seasons, respectively).

		Mouth		East 8 m		East 18 m		West 8 m		West 18 m	
		Dry	Wet	Dry	Wet	Dry	Wet	Dry	Wet	Dry	Wet
Mass flux (g m^{-2} d^{-1})	Mean	8.47	**36.32***	5.35	**9.52***	6.60	**8.99**	5.23	**10.61**	**7.48**	5.23
	Max	24.11	84.43	6.54	18.74	11.75	36.61	13.28	39.45	12.93	15.12
	Min	1.56	16.65	2.27	1.16	3.53	0.97	1.31	2.58	3.31	2.07
C_{org} flux (g m^{-2} d^{-1})	Mean	0.18	**0.61***	0.05	**0.17**	0.09	**0.21**	0.06	**0.11**	**0.12**	0.09
	Max	0.53	0.87	0.09	0.49	0.18	0.55	0.20	0.63	0.24	0.16
	Min	0.03	0.26	0.01	0.03	0.05	0.06	0.04	0.04	0.04	0.04
Total N flux (g m^{-2} d^{-1})	Mean	0.031	**0.082***	0.007	**0.031***	0.012	**0.021**	0.022	**0.033**	**0.022**	0.012
	Max	0.081	0.233	0.011	0.074	0.024	0.083	0.085	0.112	0.043	0.023
	Min	0.004	0.031	0.001	0.007	0.007	0.012	0.005	0.005	0.008	0.004
Grain	Mean	**45.53**	31.46	**62.62**	51.17	**85.96**	35.41	**86.46***	42.88	**95.34***	43.75

Size	Max	74.85	52.05	279.46	81.10	273.09	54.79	125.05	60.74	159.49	62.28
(μm)	Min	36.09	23.52	27.35	27.81	26.16	11.65	36.09	25.08	25.62	15.96
Silt and Clay %	Mean	61.67	**75.06**	52.96	**55.30**	51.69	**61.84**	38.16	**62.41***	28.65	**57.00***
	Max	79.93	96.54	72.03	77.18	77.40	88.79	58.06	79.41	40.54	81.92
	Min	49.45	50.40	25.14	35.59	37.27	47.63	25.52	43.40	22.21	39.82

3.3 Seasonal trends of mass fluxes and SPM properties

3.3.1 Mouth

Fluxes at the mouth exhibited temporal variability within each season. During April-May mass, C_{org}, and total N fluxes remained relatively stable over time. In contrast, during October-November, fluxes were significantly higher and associated with a finer grain-size distribution (Fig. 3, Table 1). The proportion of fine particles (0–20 µm) and silt (20–63 µm) increased in October-November, while the proportion of fine-to-medium sand (63–150 µm) and coarser sand (>150 µm) decreased compared to April-May (Fig. 3). The highest fluxes observed at the mouth (~70 g m^{-2} d^{-1}) directly followed a heavy rainfall event on November 2nd. At this time, the average grain size of settled material was particularly small (~24 µm), with the fine particles and silt making up ~80% of the material.

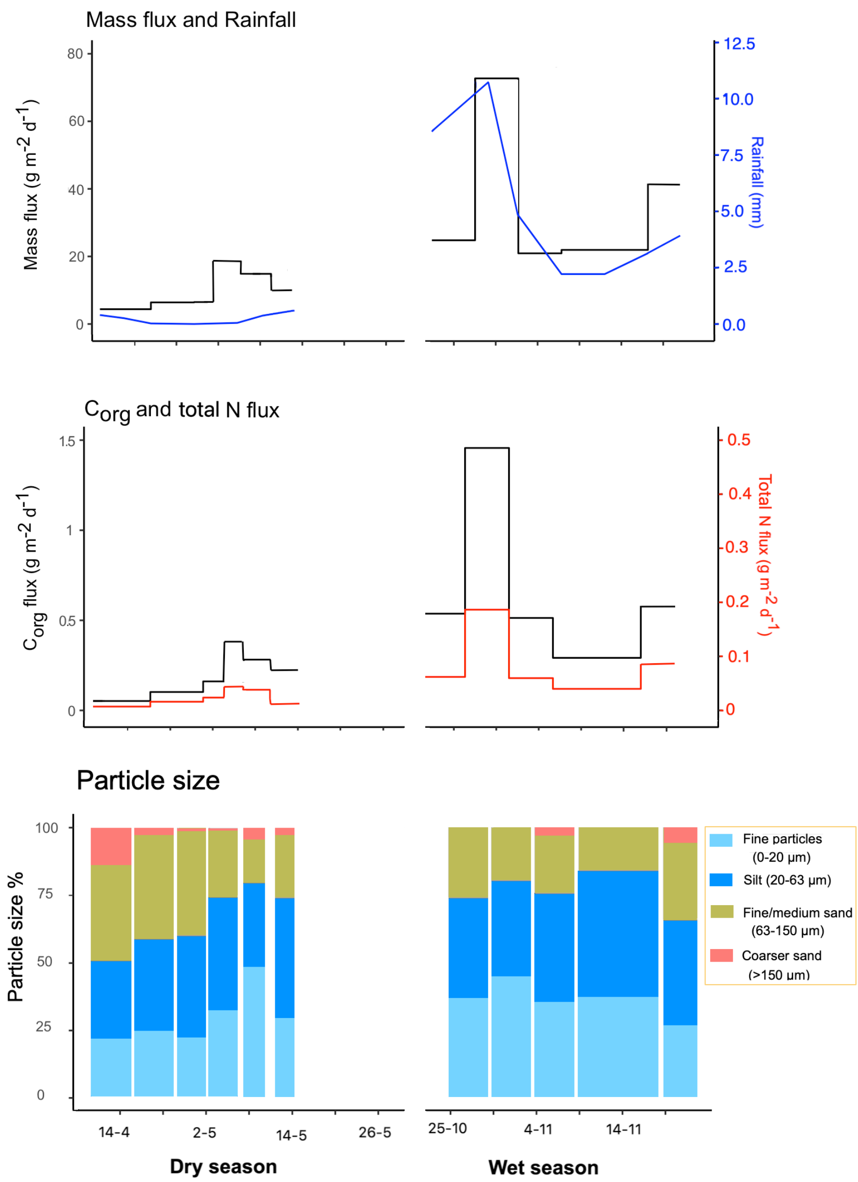

Figure 3. SPM fluxes and grain-size characteristics of the mouth in April-May (dry season) and October-November (wet season). The first panel shows mass (g m^{-2} d^{-1}) and average rainfall (mm). Second panel shows C_{org} and total N fluxes (g m^{-2} d^{-1}). Note that mass, organic carbon, and total nitrogen flux scales are different from Figure 4 and 5. Bottom panel shows the % of

fine particles (0-20 µm) silt (20-63 µm), fine-medium sand (20-150 µm) and coarser sand (>150 µm).

3.3.2 East 18 and 8 m depth

At the eastern reef, at a depth of 8 m fluxes remained relatively constant throughout most of the sampling period in April-May (Figure 4.a). Here, mass fluxes increased during May 2–16, although C_{org} and total N fluxes did not show a corresponding increase. At 18 m water depth higher variation was observed during the sampling periods. At this depth, the highest mass, C_{org} and total N fluxes were recorded towards the end of the sampling period (May 16–24). Grain-size composition did not vary during the whole sampling period at both 8 and 18 m.

In the October-November sampling period, the lowest mass, C_{org} and total N fluxes were recorded from October 25–31 (mass flux: 2–5 g m^{-2} d^{-1}, C_{org} flux: 0.06–0.1 g m^{-2} d^{-1} and total N flux: 0.004–0.01 g m^{-2} d^{-1}), while relatively high fluxes occurred from October 31–November 5 (mass flux: 12-15 g m^{-2} d^{-1}, C_{org} flux: 0.3-0.4 g m^{-2} d^{-1} and total N flux: 0.04-0.05 g m^{-2} d^{-1}), coinciding with the highest rainfall event of the sampling period (November 2). During this high-rainfall period, SPM exhibited smaller grain size, and a higher percentage of silt and clay similar to what was observed at the mouth. At both depths, the proportion of coarser sand (>150 µm) was lower in October-November compared to April-May.

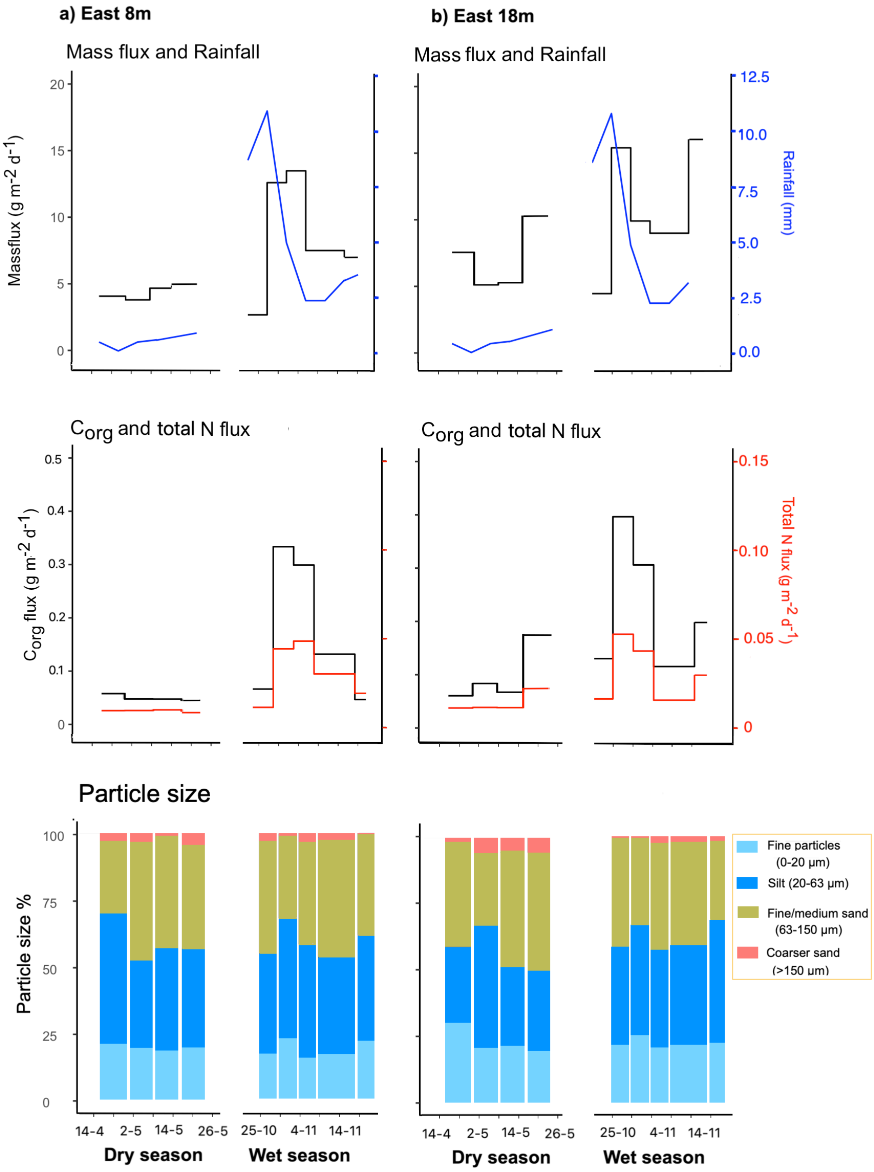

Figure 4. SPM fluxes and grain size of the a) East 8m and b) East 18m in April-May (dry season) and October-November (wet season). The upper panels show mass fluxes (g m^{-2} d^{-1}) and average rainfall (mm). Middle panels show C_{org} and total N fluxes (g m^{-2} d^{-1}). Bottom panel

shows the proportion of clay particles (0-20 µm) silt (20-63 µm), fine-medium sand (20-150 µm) and coarser sand (>150 µm).

3.3.3 West 18 m and 8 m depth

Seasonal differences at the western reef were less pronounced compared to those observed at the other locations. At 18 m, mass, C_{org}, and total N fluxes remained relatively stable both within and between seasons (Fig. 5). However, the material was coarser at this site in both seasons, with a higher proportion of coarse sand (>150 µm) than at the mouth and eastern reef. This coarser fraction was particularly present in April-May. At 8 m, mass, C_{org}, and total N fluxes showed a clear seasonal difference. During April-May, highest mass flux was recorded between May 8 and 18 (~13 g m^{-2} d^{-1}), coinciding with one of the few rainfall events in that period (May 14). In October-November, fluxes at 8 m displayed greater temporal variation, with peak values around the intense rainfall on November 2 (mass flux: 18 g m^{-2} d^{-1}; C_{org} flux: 0.3 g m^{-2} d^{-1}; total N flux: 0.05 g m^{-2} d^{-1}). Grain-size analysis showed that the percentage of fine particles (0–20 µm) and silt (20–63 µm) was higher in October-November than in April-May, particularly at 8 m. In contrast, the proportion of coarser sand was lower in October-November and generally higher at both 8 and 18 m compared to the mouth and eastern reef. At 18 m, mass fluxes were lower than at all other locations (i.e., West 8 m, East 8 m and 18 m, and the mouth).

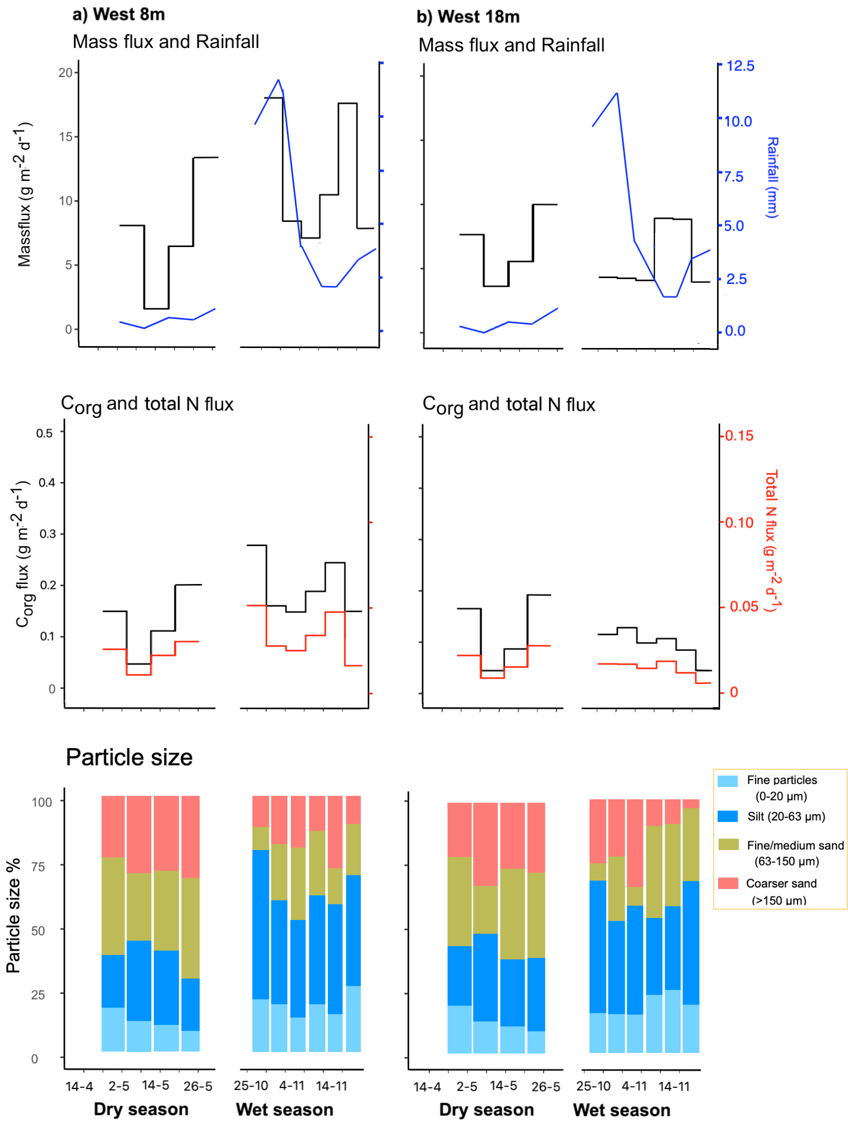

Figure 5. SPM fluxes and grain size of the a) West 8m and b) West 18m of April-May (dry season) and October-November (wet season). Upper panels show mass fluxes (g m^{-2} d^{-1}) and average rainfall (mm). Middle panels show C_{org} and total N fluxes (g m^{-2} d^{-1}). Bottom panel shows the % of clay particles (0-20 µm), silt (20-63 µm), fine-medium sand (20-150 µm) and coarse sand (>150 µm).

3.4 **Elemental composition of the suspended matter**

A principal component analysis (PCA) biplot was performed to identify broad patterns in the elemental composition of the settled material and their relationship to sampling location and season sampling period (Fig. 6). PC1 and PC2 explained 48.5% and 21.8% of the total variance, respectively. PC1 primarily reflects a location gradient, with mouth samples associated with positive PC1 values, east reef samples clustering near zero, and west reef samples towards negative PC1 values. PC2 separates seasons, with October-November (wet season) samples clustering towards positive PC2 values and April-May (dry season samples) towards negative PC2 values.

The biplot revealed four distinct element groups whose vector directions reflect these spatial and seasonal gradients. The first group, comprising Si, Mn, Ti, Al, Co and Fe (purple vectors, Fig. 6), reflects a dominant terrigenous origin probably related to runoff, with vectors pointing towards positive PC1, consistent with their elevated concentrations at the bay mouth and east reef locations. A second group, consisting of Ni, Y, Rb, Pb, and Cu (green vectors, Fig. 6), consists of elements generally associated with pollution, which were found in elevated concentrations particularly at the reef sites. A third group, defined by Br, S, Cl, Mg and K (red vectors, Fig. 6), consists of elements typical of marine organic matter and/or salts, with vectors pointing towards negative PC1, consistent with higher marine influence at the western reef locations. A fourth group comprising Sr, Ca, Zn, and Zr (teal vectors, Fig. 6) includes elements associated with marine carbonates (Ca and Sr) as well as terrigenous (Zr) and pollution (Zn) sources. As the vectors of this group are relatively short and centrally positioned in the biplot, they explain less variance and are likely not specifically driven by any single environmental factor.

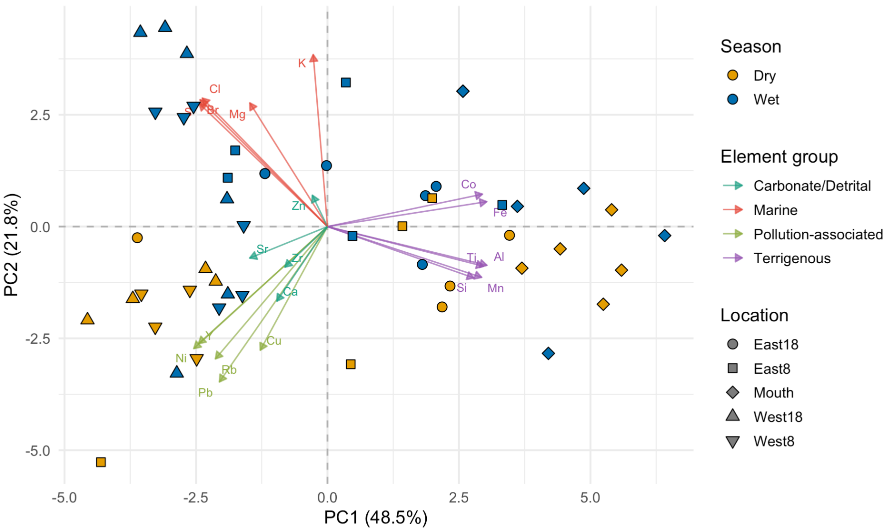

Figure 6. PCA biplot of XRF element concentrations across all sampling locations and seasons. Each point represents a sediment sample, with shape indicating location (East 8, East 18, Mouth, West 8, West 18) and color indicating season (orange: April-May (dry), blue: October-November (wet). Arrows represent element loading vectors scaled to the PC1/PC2 axes, color-coded by geochemical group: Terrigenous (purple; Mn, Ti, Al, Si, Co, Fe), Marine (red; Mg, Br, S, Cl, K), Carbonate/Detrital (teal; Ca, Sr, Zr, Zn), and Pollution-associated (green; Ni, Y, Pb, Rb, Cu). PC1 and PC2 explain 48.5% and 21.8% of the total variance, respectively.

3.4.1 Seasonal and spatial trends of elemental composition and correlations of SPM characteristics with environmental parameters

XRF analysis revealed distinct relative spatial differences in the composition of SPM (Fig. 7). Aluminum (Al), an element associated with terrigenous input, displayed the highest intensities at the mouth, and eastern reef, and the lowest at the western reef. This spatial pattern was consistent across both seasons. During October-November Al values increased following periods of intense rainfall (25 October–8 November, Fig. 2). Other terrigenous elements showed similar trends (Fig. S1). In contrast, the Pb/Al ratio, indicative of anthropogenic pollution, was highest in the western reef, lowest at the mouth and showed intermediate values in the east. This pattern held for both seasons and was consistent across other trace metal ratios (Fig. S2). The Ca/Fe ratio, reflecting the relative contribution of marine carbonate versus terrigenous inputs, exhibited a similar spatial pattern, with the highest values found in the western reef, intermediate values in the east, and the lowest at the mouth. Additionally, Ca/Fe values were higher during the dry season, showing a greater influence of marine carbonate inputs during periods of reduced runoff.

Correlations between SPM properties and environmental drivers confirmed these spatial contrasts (Fig. S4). At the mouth, mass, C_{org}, and total N fluxes were strongly intercorrelated (>0.9) and closely linked to Al, Si, Mn, and Fe, indicating a dominance of fine-grained, terrigenous material. Rainfall and wind also correlated with fluxes during October-November. At the eastern reef, fluxes were again intercorrelated, but showed weaker associations with rainfall. Correlations with Fe and Mn point to a stronger influence of silt and clay fractions. In contrast, at the western reef, fluxes correlated less with environmental drivers, but grain size showed a stronger role. Here, coarser particles were occasionally linked to higher mass and organic matter fluxes in the dry season, whereas in the wet season fluxes were more influenced by fine-grained material and terrigenous elements such as Al and Fe.

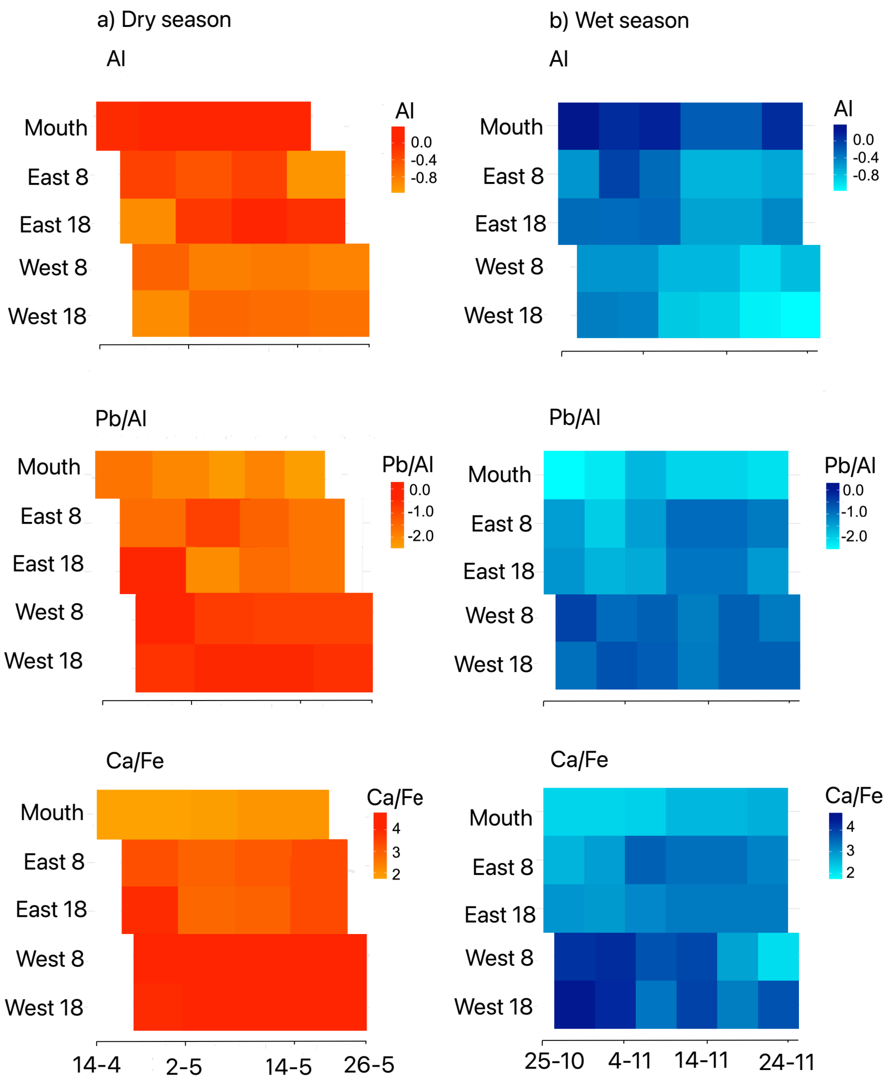

Figure 7. Heat maps of elemental intensities of Al, Pb/Al and Ca/Fe in sediment trap samples during the a) April-May (dry season in orange) and b) October-November (wet season in blue). The x-axis represents sampling dates, and the y-axis displays the five sampled locations (Mouth, East 8, East 18, West 8 and West 18). The color scale indicates the centered log-ratios (CLR) of elemental intensities for Al and log-ratios for Pb/Al and Ca/Fe.

4. Discussion

4.1 Spatial patterns

The influence of Piscadera Bay on nearshore SPM reveals clear spatial differences. Near the bay's mouth, highest mass fluxes, elevated organic content, and finest particles were found. East of the bay mouth, the suspended matter shows more impact of the bay system compared to the western reef, however less pronounced than at the mouth. This aligns with Sánchez Barranco et al. (2025), showing that bay-derived characteristics, such as dissolved-nutrient concentrations, salinity, and temperature attenuate with increasing distance from bays. Suspended matter at the eastern reef, particularly at 8 m depth, has a recognizable bay signature through elevated carbon and nitrogen content and relatively high values of elements, such as Al, Si and/ or Fe, indicating terrestrial runoff. The low current speeds and absence of a dominant directional flow at the eastern reef (8 m depth; Fig. 2) may explain the accumulation of finer material with higher organic content, creating a zone where bay influence persists due to longer particle residence times.

The western reef, positioned furthest from Piscadera Bay, reveals different patterns compared to the mouth and eastern reef. This site is characterized by less variability in fluxes of mass, C_{org}, and total N. The consistently higher Ca/Fe found here further suggest a stronger marine signal compared to the other sites, reflecting greater contributions of carbonate-rich marine particles relative to terrigenous inputs (Nizou et al., 2011). However, this location shows relatively high values of Br, S, Pb, and Ni (see also Fig. S3). This reef is exposed to a persistent west-southward current and higher wave and current energy (Fig. 2), reducing residence times of suspended particles at this site. The prevailing east-southeasterly winds observed throughout the study period suggest that swell likely approaches from the same direction, meaning the eastern reef would be relatively sheltered compared to the western reef.

Deleted: In contrast, the western

Trace metals were found at both reef sites, but values were consistently higher at the western reef, particularly for Pb and other pollution indicators (Figs. 7, S2). These trace elements suggest a complex interplay of marine biological activity and potential anthropogenic influences, with origins ranging from marine organism decomposition to maritime and industrial processes (Caballero-Gallardo et al., 2020; Fernandez et al., 2007). The presence of Pb and Ni indicates potential anthropogenic input, such as maritime activities, or influence of coastal infrastructure (Nalley et al., 2021; Fernandez et al., 2007) and corroborates high anthropogenic input (Van de Loosdrecht, submitted). In particular, the port of Schottegat, a larger and more industrialized harbor located upstream of the dominant current, may act as an additional source of trace metals to the western reef beyond Piscadera Bay itself, though the measurements used here do not allow us to distinguish between these sources.

4.2 Temporal patterns

Mass fluxes recorded at both reef sites during April-May (dry season) fall within the ranges reported for reefs worldwide that are relatively uninfluenced by human activities (i.e., 1–10 g m^{-2} d^{-1}) (Rogers, 1990). However, during October-November (wet season), this range is greatly exceeded at both reef sites (except for the western reef at 18 m water depth), with mass fluxes reaching 18–40 g m^{-2} d^{-1}. In addition, organic matter fluxes measured in reefs near other bays in Curaçao (e.g. Santa Martha) are half of the fluxes we measured in both the east (8 and 18 m) and west (8 m) during the wet season (De Jong et al., 2025).

Flux–environment correlations were stronger in the wet season, with reef fluxes 2–3 times higher during peak rainfall (Figures 4, 5, 7), consistent with reported seasonal increases (Ismail et al., 2005; Li et al., 2013) and even extreme storm-driven surges (>1000-fold; Risk, 2014). The wet-season deployment coincided with an intense rainfall event during an El Niño year, therefore the observed wet-season fluxes likely reflect episodic forcing rather than a climatological seasonal mean. Rainfall during April–May 2023 was substantially lower than the long-term monthly averages of 19.6 mm in April and 19.6 mm in May, as only 6 mm total rainfall was recorded during the sampling period. In contrast, October–November 2023 showed frequent rainfall, consistent with the climatological wet season when average monthly precipitation increases to 83.7 mm in October and 96.7 mm in November. Wind conditions also followed the expected seasonal cycle, with stronger trade winds in April–May (long-term means 31.1–32.0 km h^{-1}; measured mean ~20 m s^{-1}) and weaker, more variable winds in October–November (long-term means 24.6–25.1 km h^{-1}; measured mean ~15 m s^{-1}). Seawater temperatures exceeding 30°C during October–November were above the typical Curaçao water temperature range of 26–29°C, with shallow reef waters maintaining annual mean temperatures of 27.6–27.9°C (Bolden et al., 2026), suggesting anomalously warm marine conditions. These drier-than-normal conditions and elevated late-year temperatures are broadly consistent with Caribbean anomalies reported during strong El Niño years

Deleted: air

Deleted: 29–32

(Curaçao Weather. n.d.). High rainfall during the 2023 El Niño amplified wet-season dynamics by increasing runoff and wastewater inputs, leading to elevated fluxes (Table 1) and higher Si, Al, Fe, and Mn at the bay mouth (Figure 6). Wastewater management on the island is very limited, with only ~20% of the population connected to sewage systems (Wit et al., 2025). Additional anthropogenic inputs, including the emergency sewage overflow (Govers et al., 2014), deliver organic-rich wastewater to reefs during heavy rainfall, enhancing C_{org} and total N fluxes and strengthening their correlations with Fe and Mn (Figure 8).

The bay mouth exhibits the most pronounced correlations (Fig. S4), particularly during the wet season, where fluxes and elemental concentrations align with rainfall and wind dynamics. This suggests that the mouth functions as a conduit for terrestrial and marine material exchange, with runoff and hydrodynamics controlling SPM composition. Similar patterns have been observed on other Caribbean islands, with increased presence of elements indicating runoff such as Fe, Si and Al following rain events (Larson et al., 2015). Although Si can also indicate biogenic silica (i.e. diatoms) (Lobo et al., 2016; Palmer and Abbott, 1986), the alignment of Si with Fe and Al trends suggests it primarily reflects terrestrial runoff in our case. In addition, groundwater in Curaçao has been shown to contain elevated nitrogen and trace metal concentration in urban areas, largely due to wastewater leakage, and this contaminated groundwater discharges into coastal zones and bays, posing a risk for nutrient enrichment in these areas (Wit et al., 2025).

At the eastern reef, a similar but less pronounced trend is observed, with environmental influences becoming more prominent during October-November. In contrast, the western reef shows minimal correlations in April-May, indicating that local sedimentary processes such as resuspension likely determine SPM characteristics. During this period, limited exchange between the bay and nearshore area is expected due to a pronounced front at the bay mouth, associated with saline and warm bay waters, limiting the export of suspended material (Sánchez Barranco et al., 2025). In addition, the prevailing northwestward Caribbean Current along the southern coastline of Curaçao facilitates the transport of substances from Schottegat and the Willemstad area toward the western reef in the dry season (April-May).

Correlations increase during the wet season, when this front weakens or disappears due to rainfall-driven mixing and enhanced bay–ocean exchange. This results in increased mobilization and transport of SPM and associated elements along the southwest coast reefs (Sánchez Barranco et al., 2025; Van de Loosdrecht et al., submitted). This exchange favors the suspension of finer particles (more silt and clay), which provide larger surface area for adsorption of metals and organic matter, enriching particle-bound elements such as Cu, Zn, Pb, and Ni (Lakhan et al., 2003; Malarkey et al., 2015; Bergamaschi et al., 1997). At the same time, the dominant northwestward Caribbean Current is weakening resulting in the more frequent occurrence of cyclonic eddy conditions during these months, which can modify nearshore circulation and enhance retention or redistribution of bay-derived material along the coast (Bertoncelj et al., 2025).

East of the bay's mouth, the seasonal variability in suspended matter, both its abundance and composition, is less pronounced than at the mouth. At 8 m water depth, mass fluxes in the wet season were highest. At 18 m however, mass fluxes show no significant seasonal differences although elemental compositions vary consistently between 8 and 18 m water depths, suggesting a depth-dependent gradient in the bay's influence. This vertical variability may be driven by several processes: fine-grained particles originating from the bay or from runoff may settle closer to shore before reaching deeper waters (Mccave, 1975); differences in current speeds or directions between depths may influence the transport and resuspension of particles (Gardner et al., 2018); and other environmental conditions such as stratification or wave-induced mixing may act to retain suspended material at shallow depths.

4.3 The role of hydrodynamics

Hydrodynamics shape the conditions for suspension and settling of particulate matter at this site, with current speeds higher than those in the eastern reef (Fig. 2). The effect of current speed appears to be depth-dependent: at 8 m water depth we still observe bay or land influence, as evidenced by fluctuating fluxes during the wet season that correspond with rainfall events (Fig. 5). However, at 18 m water depth, this effect is not noticeable, suggesting diminished influence from surface runoff at greater depths. The higher current velocities affect SPM dynamics by reducing particle settling time and increasing resuspension, resulting in winnowing of fine material from the seabed and increased turbidity in the water column (De Jong et al., 2025; Prochnow et al., 1970; Cuttler et al., 2017).

Wave energy is expected to have been higher during the drier April–May period when wind speeds were stronger. Unfortunately, no wave buoy or water level data are available at or near the study site; the only tide gauge in Curaçao is located at Schottegat (Willemstad harbour), approximately 6 km away within an enclosed bay, making it unsuitable as a proxy for open-coast wave conditions at the reef sites. Safak et al. (2015) demonstrated through modeling that in areas surrounding shallow coastal bays, particularly near inlets where water circulation is restricted, tidal forces can enhance material accumulation. This process is supported by our data, showing elevated concentrations of terrigenous elements (Fig. 7) at the mouth and eastern reef site, and strong correlations between water pressure (used here as a proxy for tidal variation, Fig. S4) and both mass fluxes and coarser material, possibly reflecting both tidal transport and the preferential settling of coarser particles close to the bay mouth. This suggests that tidal forcing drives episodic pulses of suspended matter export from the bay, with coarser and heavier particles depositing preferentially near the mouth due to their faster settling velocities.

4.4 Redundancy analysis

These spatial and seasonal patterns are further supported by results of a redundancy analysis (Fig. 8), showing that approximately 49% of the total variance in SPM characteristics is explained by spatial factors including depth, distance to land, and proximity to the mouth of Piscadera Bay. Although Depth, Distance to land, and Distance to mouth are structurally linked to sampling location, low VIF values (<3) confirm these variables are not collinear, supporting the reliability of RDA1's explained variance (48.57%). In line with our results, Jouon et al. (2008) showed that fluxes of suspended particles have higher variability over space than over time. This analysis clearly differentiated the western reef (characterized by marine-associated elements) from the bay mouth (dominated by terrestrial markers), with the eastern reef showing intermediate characteristics. A portion of variance (7%) is attributable to seasonal factors, primarily driven by rainfall, wind speed, and wind direction. This multivariate approach confirms that the bay's influence follows both spatial gradients and responds to seasonal changes in environmental conditions.

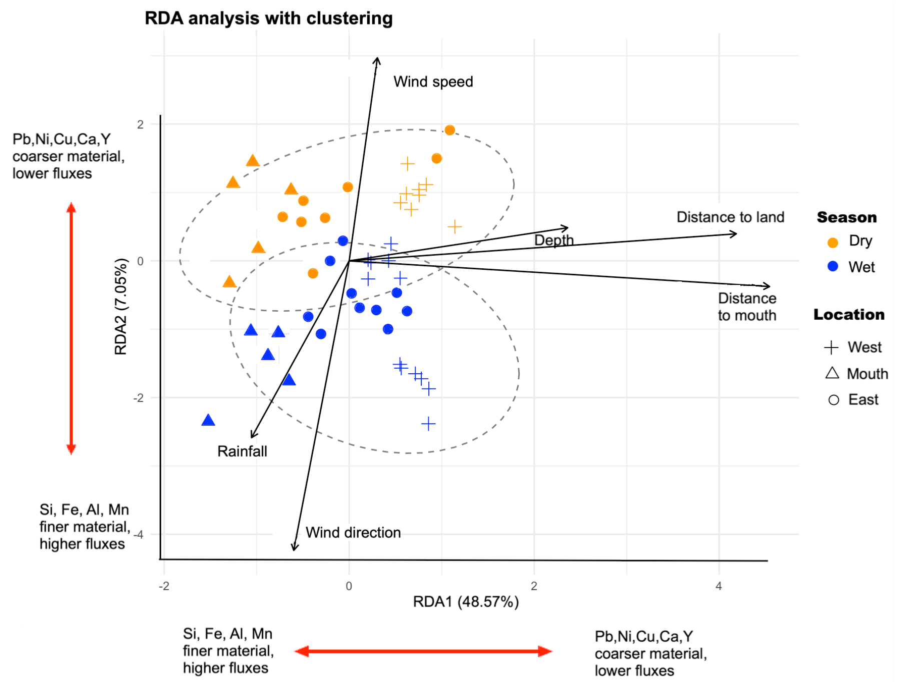

Figure 8. Redundancy analysis (RDA) biplot of sediment trap data collected from three locations in the bay (mouth, East, and West) during dry and wet seasons. Points are colored by sampling moment and shaped by location, with ellipses representing clusters at 95% confidence. RDA1 explains 48.57% of the variance and is primarily determined by depth, distance to land, and distance to the mouth, separating the locations. RDA2 accounts for only 7.05% of the variance and is driven by rainfall, wind speed, and wind direction, distinguishing between seasons

Deleted:

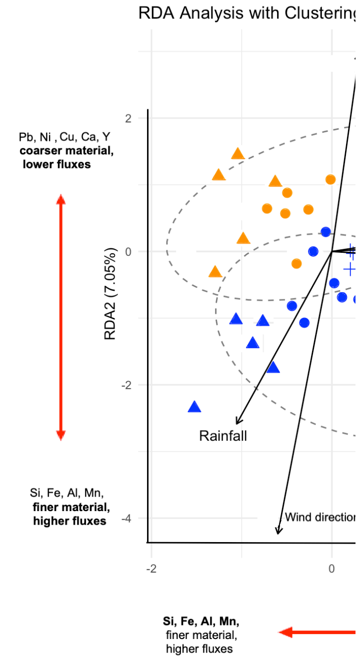

4.5 Ecological implications

The observed SPM flux patterns reveal a clear spatial gradient of terrestrial matter input, with potentially significant ecological consequences. Increased eutrophication, sedimentation, and decreased herbivory have been identified as key factors reducing coral resilience (Littler and Littler, 1998; Kuffner et al., 2008). Dutra et al. (2006) showed that SPM fluxes higher than 10 g m^{-2} d^{-1}, which in our study were recorded in both reefs during October-November, correlate with lower coral larvae survival and settlement and negatively affect coral growth. The eastern reef, more directly connected to the bay, receives higher concentrations of fine matter compared to the western reef. Fine-grained material can have detrimental effects on reef ecosystems, primarily by altering benthic conditions and preventing coral larvae settlement (Risk, 2014; Hodgson, 1990). In addition, increased water turbidity diminishes photosynthetically available radiation, which is crucial for coral and algal photosynthesis (Rogers and Ramos-Scharrón, 2022; Weber et al., 2012; Fabricius, 2005). Although elevated organic content may initially appear beneficial, chronic nutrient enrichment has been shown to exacerbate coral disease prevalence and bleaching (Aronson et al., 2003; Vega Thurber et al., 2014), while also promoting abundances of opportunistic organisms such as turf algae, macroalgae, and bacterial communities that can rapidly colonize available substrate and outcompete corals for space and light resources, ultimately leading to phase shifts from coral-dominated to algae-dominated reef systems (Gorgula and Connell, 2004; Vermeij et al., 2010).

In the past decades, studies have shown the effect of these bays in nearby reefs and the properties of the water column. For instance, Govers et al. (2014) demonstrated that other ecosystems, such as seagrass beds, are threatened by eutrophication resulting from emergency wastewater overflow and coastal housing near these bays. Also, recent studies have proven the presence of organic chemical pollution around bays in Curaçao as indicators of waste water and industrial pollution (De Jong et al., 2025). The SPM dynamics observed in this study provide important insights into the environmental conditions affecting the reefs surrounding Piscadera Bay, which have undergone significant benthic cover transformations in recent decades. In-situ studies conducted around Piscadera Bay have demonstrated that turf algae and microalgae take up nutrients more efficiently than corals after episodic release by plumes from the bay during rainfall events, thereby providing these algae with a competitive advantage over corals (Den Haan et al., 2016; Vermeij et al., 2010). While these observations are consistent with long-term benthic shifts documented at these reefs, the present study cannot resolve whether current SPM regimes initiated these changes or primarily contribute to maintaining the existing algal-dominated state.

Our study also shows relatively high levels of elements such as Fe, Al and Mn, which corroborates with the land-derived anthropogenic signatures found along the southwest coast of Curaçao (Van de Loosdrecht, submitted). Reefs close to land areas with increasing altered surface (i.e., the proportion of the onshore watershed that was occupied by human-modified surfaces, including habitations, commercial developments, and roads that can be associated with increased risk for urban runoff and pollution) showed higher loading of pollutants, and this correlation was enhanced with higher precipitation (Van de Loosdrecht, submitted). While XRF measurements are semi-quantitative and primarily reflect relative abundances, they are useful to indicate terrestrial runoff. Accordingly, XRF-derived elemental intensities and ratios are interpreted as relative spatial and temporal variations rather than absolute concentrations and therefore cannot be directly compared to established toxicity thresholds. Nevertheless, elevated concentrations of terrestrially derived material can be harmful to corals and may promote growth of cyanobacteria and turf algae (Kelly, 2013; Esslemont, 1999). Turf algae, which can rapidly colonize newly available substratum, have become dominant on many coral reefs worldwide (Sandin et al., 2008b), further indicating ecosystem shifts in response to environmental changes. This pattern has also been seen over the past 40 years in the reefs of this study. Both the western and eastern reefs have experienced noticeable decrease in coral cover, now predominantly featuring turf algae and increased abundance of cyanobacterial mats, being more pronounced in the eastern reef, which is more directly subjected to bay-derived material (Sandin et al., 2022; De Bakker et al., 2016; Van Duyl, 1985).

The western reef faces different conditions, characterized by trace-metal values suggesting alternative environmental pressures. Although Pb and Ni show spatial patterns consistent with anthropogenic inputs, spatial co-variation alone does not allow a definitive identification of the source. In marine systems, trace metals can associate not only with terrigenous clays but also with marine organic matter, which acts as an efficient scavenger in the water column (e.g., Salomons and Förstner, 1984). The clustering of Pb and Ni with marine or organic-associated vectors therefore suggests that their distribution may reflect both source inputs and post-depositional partitioning processes. We therefore distinguish between metal origin and transport pathway and interpret the observed enrichments as consistent with, rather than diagnostic of, sewage or maritime sources. The west-southward current measured at the western reef (Figure 2) is consistent with the eddy-like circulation described and predicted for this period by Bertoncelj et al. (2025) , playing a role in dispersing bay-derived materials away from nearshore areas, reducing residence times and potentially limiting the accumulation of terrestrial SPM at this site. However, this eddy-driven recirculation may simultaneously act as a delivery mechanism for anthropogenic contaminants transported along the urbanized coastline, helping to explain the elevated trace metal signals (Pb, Ni, Cu) observed preferentially at the western reef. However, the limited duration of dry-season current measurements restricts quantitative validation of this mechanism. This same dispersal mechanism also facilitates the broader distribution of potential contaminants across the reef system. The contrasting hydrodynamic conditions between sites may explain observed differences in reef community composition, where the eastern reef, characterized by lower current velocities (Fig.2) and thus longer residence times shows greater ecological degradation compared to the western reef (De Bakker et al., 2017; Sandin et al., 2022), which experiences higher current velocities (Fig.2) and more effective flushing by the main current system. This differential exposure to terrestrial materials represents a critical factor in understanding current reef composition and predicting future development patterns (Fig. 9).

While the semi-quantitative XRF measurements of Ni, Cu, and Pb cannot be definitively classified as toxic, their presence indicates enhanced anthropogenic-related matter fluxes (Fernandez et al., 2007; Caballero-Gallardo et al., 2020). For example, Ni can limit calcium available for growth, affect respiration, reduce coral larvae settlement and reproduction, and negatively impact other key reef organisms such as anemones or sea urchins (Méndez et al., 2021; Reichelt-Brushett and Hudspith, 2016; Reichelt-Brushett and Harrison, 2005; Nalley et al., 2021). Pb can likewise impair coral growth and photosynthesis of corals and macroalgae (Baumann et al., 2009). Our findings align with studies suggesting that chronic exposure to certain pollutants may contribute to long-term reef degradation (Jackson et al., 2014).

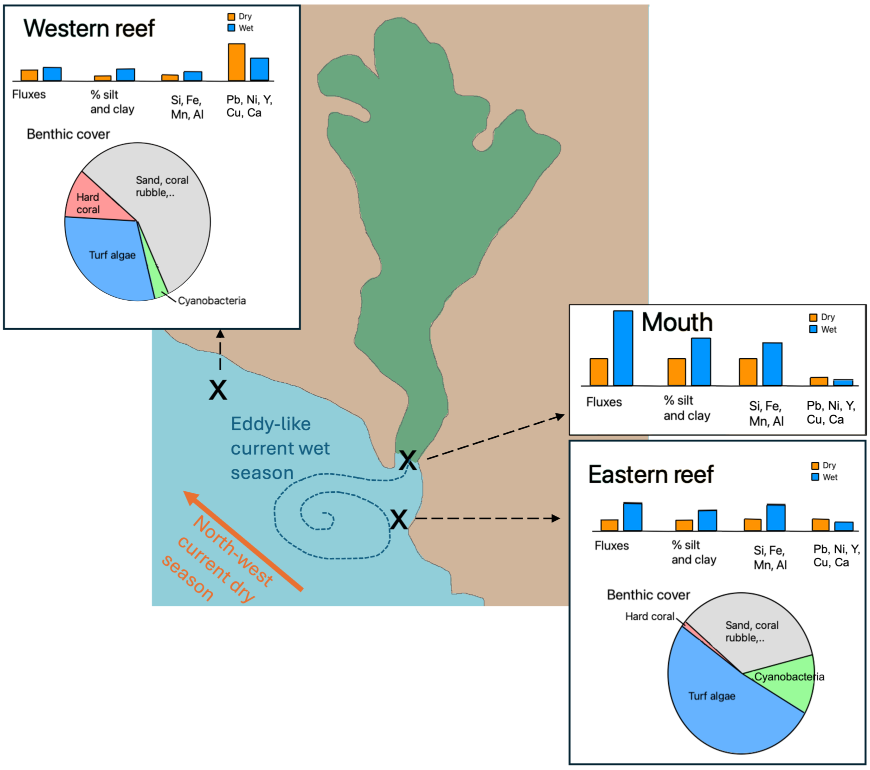

Figure 9. Summary of the spatial and seasonal variability in SPM characteristics and benthic cover (De Bakker et al., 2017) in reefs nearby Piscadera Bay. (Graphical abstract)

The interpretation of SPM fluxes and composition in shallow reef environments is subject to several constraints. Sediment trap deployments integrate both background conditions and episodic events, and the wet-season deployment coincided with an intense rainfall event during an El Niño year. Consequently, the reported wet-season fluxes should be interpreted as event-integrated snapshots rather than seasonal or annual baselines. In addition, elemental compositions derived from XRF are semi-quantitative and used to assess relative spatial patterns and source influences; methods such as ICP-MS could be used to quantify absolute concentrations and determine whether toxicity thresholds are reached. Finally, while spatial gradients in elemental composition suggest differing transport and retention processes among reef sites, definitive source attribution and mechanistic explanations require complementary approaches, including absolute concentration measurements, hydrodynamic modelling, studying different bay systems and biological indicators.

5 Conclusions

This study highlights the spatial and seasonal dynamics of suspended particulate matter near Piscadera Bay, one of over 35 bays and water inlets along Curaçao's south coast that are subject to varying degrees of human impact. Seasonal differences show that dry-season SPM dynamics are controlled by localized factors (tides, resuspension, currents), while wet-season conditions are dominated by rainfall, wind, and enhanced hydrodynamics.

Coral reefs near bay mouths are particularly influenced by bay-derived inputs during wet-season runoff. The RDA reveals a spatial gradient from the bay mouth to the western reef, with the eastern reef showing intermediate characteristics (Fig. 8), highlighting the role of bay-ocean exchange in transport processes. The eastern reef experiences prolonged exposure to terrestrial material due to proximity and slower dispersal, potentially intensifying ecological stress, while the western reef benefits from rapid material dispersal.

Deleted: ,

Deleted: with strengthening west-to-east correlations

The threat to reefs stems from increased pollutant loads and persistent fine particles that reduce light availability and transport harmful elements. In sheltered areas, slower hydrodynamic exchange prolongs these effects, altering material quality and quantity reaching reefs with important implications for reef health and resilience. Future research should compare SPM characteristics across multiple bays and include ecotoxicological assays to identify elements posing the greatest risk—essential for informing targeted mitigation strategies and evidence-based coastal management.

Author Contributions

Virginia Sánchez Barranco: conceptualization, sampling, laboratory analysis, statistical analysis, and writing the first draft. Nienke C.J. van de Loosdrecht: conceptualization, sampling, laboratory analysis, and contribution to the final manuscript. Furu Mienis, Jasper M. de Goeij, and Lennart de Nooijer: conceptualization, funding acquisition, and contribution to the final manuscript. Rick Hennekam, Gert-Jan Reichart, and Jan-Berend Stuut: contribution to the final manuscript.

Competing Interests

The authors declare no competing interests.

Acknowledgements

This publication is part of the project "Land, Sea, and Society: Linking terrestrial pollutants and inputs to nearshore coral reef growth to identify novel conservation options for the Dutch Caribbean (SEALINK)" with project number NWOCA.2019.003 of the research program "Caribbean Research: a Multidisciplinary Approach" which is (partly) financed by the Dutch Research Council (NWO). We heartily thank the project leader Mark Vermeij for facilitating our work at CARMABI. We thank Vesna Bertoncelj for helping processing the current data collected with the ADCP. We heartily thank Petra Visser for her advice. We greatly acknowledge the team of CARMABI that helped sampling. We also want to thank Jeroen Kooijman for his hard work and expert abilities in the XRF analysis. Finally, we gratefully thank Fay Diederiks and Julia Piaskowy for their help during fieldwork.

Data

The data supporting this study are openly available and can be accessed via the DOI: https://dataportal.nioz.nl/doi/10.25850/nioz/7b.b.2j

References

Curaçao Weather. n.d., last access: 5-9-2024.
Anthony, K. R.: Coral suspension feeding on fine particulate matter, Journal of Experimental Marine Biology and Ecology, 232, 85-106, 1999.
Anthony, K. R. and Fabricius, K. E.: Shifting roles of heterotrophy and autotrophy in coral energetics under varying turbidity, Journal of experimental marine biology and ecology, 252, 221-253, 2000.
Anthony, K. R., Kline, D. I., Diaz-Pulido, G., Dove, S., and Hoegh-Guldberg, O.: Ocean acidification causes bleaching and productivity loss in coral reef builders, Proceedings of the National Academy of Sciences, 105, 17442-17446, 2008.
Aronson, R. B., Bruno, J. F., Precht, W. F., Glynn, P. W., Harvell, C. D., Kaufman, L., Rogers, C. S., Shinn, E. A., and Valentine, J. F.: Causes of coral reef degradation, Science, 302, 1502-1504, 2003.
Bak, R. P.: Coral reefs and their zonation in Netherlands Antilles: modern and ancient reefs, 1977.
Baumann, H. A., Morrison, L., and Stengel, D. B.: Metal accumulation and toxicity measured by PAM—chlorophyll fluorescence in seven species of marine macroalgae, Ecotoxicology and Environmental Safety, 72, 1063-1075, 2009.
Bergamaschi, B. A., Tsamakis, E., Keil, R. G., Eglinton, T. I., Montluçon, D. B., and Hedges, J. I.: The effect of grain size and surface area on organic matter, lignin and carbohydrate concentration, and molecular compositions in Peru Margin sediments, Geochimica et Cosmochimica Acta, 61, 1247-1260, 1997.

Berry, K. L., Seemann, J., Dellwig, O., Struck, U., Wild, C., and Leinfelder, R. R.: Sources and spatial distribution of heavy metals in scleractinian coral tissues and sediments from the Bocas del Toro Archipelago, Panama, Environmental monitoring and assessment, 185, 9089-9099, 2013.

Bertoncelj, V., Mienis, F., Stocchi, P., and van Sebille, E.: Flow patterns, hotspots, and connectivity of land-derived substances at the sea surface of Curaçao in the southern Caribbean, Ocean Science, 21, 945-964, 2025.

Bertrand, S., Tjallingii, R., Kylander, M. E., Wilhelm, B., Roberts, S. J., Arnaud, F., Brown, E., and Bindler, R.: Inorganic geochemistry of lake sediments: A review of analytical techniques and guidelines for data interpretation, Earth-Science Reviews, 249, 104639, 2024.

Bhuyan, M. S., Jenzri, M., and Adikari, D.: Impacts of sedimentation on coral health and reef ecosystems: A comprehensive review, Marine Pollution Bulletin, 221, 118480, 2025.

Bolden, I. W., Timmerman, A. H., Clark, D. R., Belanger, B. K., Oster, J. L., Salas-Saavedra, M., and Niespolo, E. M.: Monitoring coral reef metabolism under changing oceans–Novel insights from seawater stable carbon isotopes, Journal of Geophysical Research: Biogeosciences, 131, e2025JG009416, 2026.

Burke, L. and Maidens, J.: Reefs at Risk in the Caribbean, 2004.

Burke, L., Reytar, K., Spalding, M., and Perry, A.: Reefs at risk revisited, Washington, DC: World Resources Institute (WRI)2011.

Caballero-Gallardo, K., Alcala-Orozco, M., Barraza-Quiroz, D., De la Rosa, J., and Olivero-Verbel, J.: Environmental risks associated with trace elements in sediments from Cartagena Bay, an industrialized site at the Caribbean, Chemosphere, 242, 125173, 2020.

Cuttler, M. V., Lowe, R. J., Falter, J. L., and Buscombe, D.: Estimating the settling velocity of bioclastic sediment using common grain-size analysis techniques, Sedimentology, 64, 987-1004, 2017.

D'Sa, E. J. and Ko, D. S.: Short-term influences on suspended particulate matter distribution in the northern Gulf of Mexico: Satellite and model observations, Sensors, 8, 4249-4264, 2008.

De Bakker, D. M., Meesters, E. H., Bak, R. P., Nieuwland, G., and Van Duyl, F. C.: Long-term shifts in coral communities on shallow to deep reef slopes of Curaçao and Bonaire: are there any winners?, Frontiers in Marine Science, 3, 247, 2016.

De Bakker, D. M., Van Duyl, F. C., Bak, R. P., Nugues, M. M., Nieuwland, G., and Meesters, E. H.: 40 Years of benthic community change on the Caribbean reefs of Curaçao and Bonaire: the rise of slimy cyanobacterial mats, Coral Reefs, 36, 355-367, 2017.

De Carlo, E. H., Hoover, D. J., Young, C. W., Hoover, R. S., and Mackenzie, F. T.: Impact of storm runoff from tropical watersheds on coastal water quality and productivity, Applied Geochemistry, 22, 1777-1797, 2007.

de Jong, C., van Os, I., Sepúlveda-Rodríguez, G., de Baat, M. L., and Schoepf, V.: High-resolution temporal assessment of physicochemical variability and water quality in tropical semi-enclosed bays and coral reefs, Science of the Total Environment, 968, 178810, 2025.

Debrot, A., Kuenen, M., and Dekker, K.: Recent declines in the coral fauna of the Spaanse Water, Curaçao, Netherlands Antilles, Bulletin of marine science, 63, 571-580, 1998.

Den Haan, J., Huisman, J., Brocke, H. J., Goehlich, H., Latijnhouwers, K. R., Van Heeringen, S., Honcoop, S. A., Bleyenberg, T. E., Schouten, S., and Cerli, C.: Nitrogen and phosphorus uptake rates of different species from a coral reef community after a nutrient pulse, Scientific reports, 6, 28821, 2016.

Dutra, L., Kikuchi, R., and Leão, Z.: Effects of sediment accumulation on reef corals from Abrolhos, Bahia, Brazil, Journal of Coastal Research, 633-638, 2006.

Dutra, L., Haywood, M. D., Singh, S. S., Piovano, S., Ferreira, M., Johnson, J. E., Veitayaki, J., Kininmonth, S. J., and Morris, C. W.: Effects of climate change on corals relevant to the Pacific Islands, Pacific marine climate change report card, 132-158, 2018.

Erftemeijer, P. L., Riegl, B., Hoeksema, B. W., and Todd, P. A.: Environmental impacts of dredging and other sediment disturbances on corals: a review, Marine pollution bulletin, 64, 1737-1765, 2012.

Esslemont, G.: Heavy metals in corals from Heron Island and Darwin harbour, Australia, Marine Pollution Bulletin, 38, 1051-1054, 1999.

Fabricius, K. E.: Effects of terrestrial runoff on the ecology of corals and coral reefs: review and synthesis, Marine pollution bulletin, 50, 125-146, 2005.

Fabricius, K. E. and Dommisse, M.: Depletion of suspended particulate matter over coastal reef communities dominated by zooxanthellate soft corals, Marine Ecology Progress Series, 196, 157-167, 2000.

Fernandez, A., Singh, A., and Jaffé, R.: A literature review on trace metals and organic compounds of anthropogenic origin in the Wider Caribbean Region, Marine Pollution Bulletin, 54, 1681-1691, 2007.

Gardner, W. D., Richardson, M. J., and Mishonov, A. V.: Global assessment of benthic nepheloid layers and linkage with upper ocean dynamics, Earth and Planetary Science Letters, 482, 126-134, 2018.

Gorgula, S. K. and Connell, S. D.: Expansive covers of turf-forming algae on human-dominated coast: the relative effects of increasing nutrient and sediment loads, Marine Biology, 145, 613-619, 2004.

Govers, L. L., Lamers, L. P., Bouma, T. J., de Brouwer, J. H., and van Katwijk, M. M.: Eutrophication threatens Caribbean seagrasses–An example from Curaçao and Bonaire, Marine pollution bulletin, 89, 481-486, 2014.

Guzmán, H. M. and Jiménez, C. E.: Contamination of coral reefs by heavy metals along the Caribbean coast of Central America (Costa Rica and Panama), Marine Pollution Bulletin, 24, 554-561, 1992.

Heiskanen, A.-S. and Tallberg, P.: Sedimentation and particulate nutrient dynamics along a coastal gradient from a fjord-like bay to the open sea, Biological, Physical and Geochemical Features of Enclosed and Semi-enclosed Marine Systems: Proceedings of the Joint BMB 15 and ECSA 27 Symposium, 9–13 June 1997, Åland Islands, Finland, 127-140,

Hodgson, G.: Sediment and the settlement of larvae of the reef coral Pocillopora damicornis, Coral Reefs, 9, 41-43, 1990.

Hofker, J.: The foraminifera of Piscadera Bay, Curacao, Studies on the Fauna of Curacao and other Caribbean Islands, 35, 1-62, 1971.

Ismail, M., Kimura, T., Suzuki, Y., and Tsuchiya, M.: Seasonal and spatial variations of total mass flux around coral reefs in the southern Ryukyus, Japan, Journal of oceanography, 61, 631-644, 2005.

Jackson, J., Donovan, M., Cramer, K., and Lam, V.: Status and trends of Caribbean coral reefs: 1970-2012, Gland, Switzerland: Global Coral Reef Monitoring Network; International ...2014.

Jouon, A., Ouillon, S., Douillet, P., Lefebvre, J. P., Fernandez, J. M., Mari, X., and Froidefond, J.-M.: Spatio-temporal variability in suspended particulate matter concentration and the role of aggregation on size distribution in a coral reef lagoon, Marine Geology, 256, 36-48, 2008.

Kelly, L. E. W.: Coral reef microbes: the influences of benthic primary producers, nutrient availability, and anthropogenic stressors on community structure and metabolism, University of California, San Diego2013.

Korte, L. F., Brummer, G.-J. A., Van Der Does, M., Guerreiro, C. V., Hennekam, R., Van Hateren, J. A., Jong, D., Munday, C. I., Schouten, S., and Stuut, J.-B. W.: Downward particle fluxes of biogenic matter and Saharan dust across the equatorial North Atlantic, Atmospheric Chemistry and Physics, 17, 6023-6040, 2017.

Lakhan, V., Cabana, K., and LaValle, P.: Relationship between grain size and heavy metals in sediments from beaches along the coast of Guyana, Journal of Coastal Research, 600-608, 2003.

Larson, R. A., Brooks, G. R., Devine, B., Schwing, P. T., Holmes, C. W., Jilbert, T., and Reichart, G.-J.: Elemental signature of terrigenous sediment runoff as recorded in coastal salt ponds: US Virgin Islands, Applied Geochemistry, 63, 573-585, 2015.
Li, X.-b., Huang, H., Lian, J.-s., Liu, S., Huang, L.-m., and Yang, J.-h.: Spatial and temporal variations in sediment accumulation and their impacts on coral communities in the Sanya Coral Reef Reserve, Hainan, China, Deep Sea Research Part II: Topical Studies in Oceanography, 96, 88-96, 2013.
Lobo, E. A., Heinrich, C. G., Schuch, M., Wetzel, C. E., and Ector, L.: Diatoms as bioindicators in rivers, River algae, 245-271, 2016.
Malarkey, J., Baas, J. H., Hope, J. A., Aspden, R. J., Parsons, D. R., Peakall, J., Paterson, D. M., Schindler, R. J., Ye, L., and Lichtman, I. D.: The pervasive role of biological cohesion in bedform development, Nature communications, 6, 6257, 2015.
McCAVE, I.: Vertical flux of particles in the ocean, Deep Sea Research and Oceanographic Abstracts, 491-502,
Méndez, S., Ruepert, C., Mena, F., and Cortés, J.: Accumulation of heavy metals (Cd, Cr, Cu, Mn, Pb, Ni, Zn) in sediments, macroalgae (Cryptonemia crenulata) and sponge (Cinachyrella kuekenthali) of a coral reef in Moín, Limon, Costa Rica: An ecotoxicological approach, Marine Pollution Bulletin, 173, 113159, 2021.
Publications and Reports: https://www.meteo.cw/publications_reports.php?Lang=Eng&St=TNCC, last access: 7 July 2025.
Nalley, E. M., Tuttle, L. J., Barkman, A. L., Conklin, E. E., Wulstein, D. M., Richmond, R. H., and Donahue, M. J.: Water quality thresholds for coastal contaminant impacts on corals: A systematic review and meta-analysis, Science of the Total Environment, 794, 148632, 2021.
Nizou, J., Hanebuth, T. J., and Vogt, C.: Deciphering signals of late Holocene fluvial and aeolian supply from a shelf sediment depocentre off Senegal (north-west Africa), Journal of Quaternary Science, 26, 411-421, 2011.
Palmer, A. J. and Abbott, W. H.: Diatoms as indicators of sea-level change, in: Sea-level Research: a Manual for the Collection and Evaluation of Data, Springer, 457-487, 1986.
Prochnow, D., Engelhardt, C., and Bungartz, H.: Dynamics of settling velocity distribution of suspended particulate matter during sedimen-tation processes in rivers, WIT Transactions on Ecology and the Environment, 33, 1970.
Ramos-Scharrón, C. E. and MacDonald, L. H.: Measurement and prediction of sediment production from unpaved roads, St John, US Virgin Islands, Earth Surface Processes and Landforms: The Journal of the British Geomorphological Research Group, 30, 1283-1304, 2005.
Reichelt-Brushett, A. and Hudspith, M.: The effects of metals of emerging concern on the fertilization success of gametes of the tropical scleractinian coral Platygyra daedalea, Chemosphere, 150, 398-406, 2016.
Reichelt-Brushett, A. J. and Harrison, P. L.: The effect of selected trace metals on the fertilization success of several scleractinian coral species, Coral reefs, 24, 524-534, 2005.
Restrepo, J. D., Park, E., Aquino, S., and Latrubesse, E. M.: Coral reefs chronically exposed to river sediment plumes in the southwestern Caribbean: Rosario Islands, Colombia, Science of the Total Environment, 553, 316-329, 2016.
Rijsberman, F. and Westmacott, S.: Costeffectiveness analysis of coral reef management and protection: A case study of Curacao, Integrated coastal zone management of coral reefs: Decision support modeling. The International Bank for Reconstruction and Development, The World Bank, Washington DC, USA, 49-66, 2000.
Ringuet, S. and Mackenzie, F. T.: Controls on nutrient and phytoplankton dynamics during normal flow and storm runoff conditions, southern Kaneohe Bay, Hawaii, Estuaries, 28, 327-337, 2005.

Risk, M. J.: Assessing the effects of sediments and nutrients on coral reefs, Current Opinion in Environmental Sustainability, 7, 108-117, 2014.

Rogers, C. S.: Responses of coral reefs and reef organisms to sedimentation, Marine ecology progress series. Oldendorf, 62, 185-202, 1990.

Rogers, C. S. and Ramos-Scharrón, C. E.: Assessing effects of sediment delivery to coral reefs: A Caribbean watershed perspective, Frontiers in Marine Science, 8, 773968, 2022.

Salomons, W. and Förstner, U.: Metals in the Hydrocycle, Springer Science & Business Media2012.

Sánchez Barranco, V., Schellenberg, L., Mienis, F., Brussaard, C. P., Haas, A. F., and de Nooijer, L. J.: Seasonal Changes in Bay Water Column Properties and Their Influence on the Distribution of Dissolved and Particulate Substances Along the South Coast of Curaçao (Caribbean Sea), Marine pollution bulletin, 10.25850/nioz7b.b.0h, 2025.

Sandin, S. A., Sampayo, E. M., and Vermeij, M. J.: Coral reef fish and benthic community structure of Bonaire and Curaçao, Netherlands Antilles, Caribbean Journal of Science, 44, 137-144, 2008a.

Sandin, S. A., Alcantar, E., Clark, R., de León, R., Dilrosun, F., Edwards, C. B., Estep, A. J., Eynaud, Y., French, B. J., and Fox, M. D.: Benthic assemblages are more predictable than fish assemblages at an island scale, Coral reefs, 41, 1031-1043, 2022.

Sandin, S. A., Smith, J. E., DeMartini, E. E., Dinsdale, E. A., Donner, S. D., Friedlander, A. M., Konotchick, T., Malay, M., Maragos, J. E., and Obura, D.: Baselines and degradation of coral reefs in the Northern Line Islands, PloS one, 3, e1548, 2008b.

Storlazzi, C. D., Field, M. E., and Bothner, M. H.: The use (and misuse) of sediment traps in coral reef environments: theory, observations, and suggested protocols, Coral Reefs, 30, 23-38, 2011.

Storlazzi, C. D., Norris, B. K., and Rosenberger, K. J.: The influence of grain size, grain color, and suspended-sediment concentration on light attenuation: Why fine-grained terrestrial sediment is bad for coral reef ecosystems, Coral Reefs, 34, 967-975, 2015.

Tuttle, L. J. and Donahue, M. J.: Effects of sediment exposure on corals: a systematic review of experimental studies, Environmental Evidence, 11, 4, 2022.

Van Der Does, M., Korte, L. F., Munday, C. I., Brummer, G.-J. A., and Stuut, J.-B. W.: Particle size traces modern Saharan dust transport and deposition across the equatorial North Atlantic, Atmospheric Chemistry and Physics, 16, 13697-13710, 2016.

Van Duyl, F. C.: Atlas of the Living Reefs of Cura «; ao and Bonaire (Netherlands Antilles), Foundation for Scientific Research in Surinam and the Netherlands Antilles, 117, 1985.

Vega Thurber, R. L., Burkepile, D. E., Fuchs, C., Shantz, A. A., McMinds, R., and Zaneveld, J. R.: Chronic nutrient enrichment increases prevalence and severity of coral disease and bleaching, Global change biology, 20, 544-554, 2014.

Vermeij, M. J., van Moorselaar, I., Engelhard, S., Hörnlein, C., Vonk, S. M., and Visser, P. M.: The effects of nutrient enrichment and herbivore abundance on the ability of turf algae to overgrow coral in the Caribbean, PloS one, 5, e14312, 2010.

Wagenaar Hummelinck, P.: Marine localities, Studies on the Fauna of Curaçao and other Caribbean Islands, 51, 1-68, 1977.

Weber, M., Lott, C., and Fabricius, K.: Sedimentation stress in a scleractinian coral exposed to terrestrial and marine sediments with contrasting physical, organic and geochemical properties, Journal of experimental marine biology and ecology, 336, 18-32, 2006.

Weber, M., De Beer, D., Lott, C., Polerecky, L., Kohls, K., Abed, R. M., Ferdelman, T. G., and Fabricius, K. E.: Mechanisms of damage to corals exposed to sedimentation, Proceedings of the National Academy of Sciences, 109, E1558-E1567, 2012.

Weltje, G. J. and Tjallingii, R.: Calibration of XRF core scanners for quantitative geochemical logging of sediment cores: Theory and application, Earth and Planetary Science Letters, 274, 423-438, 2008.

Wit, M. R., van Egmond, J.-L., Kruijssen, T. P., Bense, V. F., and van Breukelen, B. M.: Hydrogeochemical signatures and human impact: A comprehensive analysis of groundwater quality on the semi-arid island of Curaçao, Journal of Hydrology: Regional Studies, 60, 102555, 2025.

Zhang, J., Zhou, F., Chen, C., Sun, X., Shi, Y., Zhao, H., and Chen, F.: Spatial distribution and correlation characteristics of heavy metals in the seawater, suspended particulate matter and sediments in Zhanjiang Bay, China, PLoS One, 13, e0201414, 2018.